

## RESEARCH ARTICLE

# Increasing the illumination slowly over several weeks protects against light damage in the eyes of the crustacean *Mysis relicta*

Martta L. M. Viljanen<sup>1,\*</sup>, Noora E. Nevala<sup>1,2</sup>, Cecilia L. Calais-Granö<sup>1</sup>, K. Magnus W. Lindström<sup>3</sup> and Kristian Donner<sup>1</sup>

**ABSTRACT**

The eyes of two glacial-relict populations of opossum shrimp *Mysis relicta* inhabiting the different photic environments of a deep, dark-brown freshwater lake and a variably lit bay of the Baltic Sea differ in their susceptibility to functional depression from strong light exposures. The lake population is much more vulnerable than the sea population. We hypothesized that the difference reflects physiological adaptation mechanisms operating on long time scales rather than genetically fixed differences between the populations. To test this, we studied how acclimation to ultra-slowly increased illumination (on time scales of several weeks to months) affected the resilience of the eyes to bright-light exposures. Light responses of whole eyes were measured by electroretinography, the visual-pigment content of single rhabdoms by microspectrophotometry and the structural integrity of photoreceptor cells by electron microscopy (EM). Slow acclimation mitigated and even abolished the depression of photoresponsiveness caused by strong light exposures, making a dramatic difference especially in the lake animals. Still, acclimation in the sea animals was faster and the EM studies suggested intrinsic differences in the dynamics of microvillar membrane cycling. In conclusion, we report a novel form of physiological adaptation to general light levels, effective on the time scale of seasonal changes. It explains part but not all of the differences in light tolerance between the lake and sea populations.

**KEY WORDS:** Compound eye, Visual adaptation, Ecophysiology, Rhodopsin, Metarhodopsin, Rhabdom

**INTRODUCTION**

Photoreceptors are susceptible to damage from the very functions they are designed to perform most efficiently: photon capture and signal amplification. Light absorption and phototransduction are associated with the release of large amounts of energy liable to cause damage through oxidative stress and several other possible mechanisms (Glickman, 2002; Organisciak and Vaughan, 2010; Insausti et al., 2013). The threat of light damage to eyes is universal and especially acute when eyes tuned for exquisite sensitivity are exposed to bright light. Within certain limits, homeostasis is maintained or quickly restored by known physiological recovery mechanisms but, beyond that, various degrees of injury may occur. In crustacean rhabdoms, the well-ordered microvillar pattern

will undergo structural changes ranging from minor irregularities to severe and persistent disorganization (Loew, 1976; Bloom and Atwood, 1981; Nilsson, 1982; Lindström and Nilsson, 1983; Meyer-Rochow, 2001). Known functional correlates are decreases in the electrophysiologically recorded responsiveness of the eye, ranging from near-normal light–dark adaptation to long-lasting severe depression or loss of light sensitivity (Lindström and Nilsson, 1988), as well as behavioural changes (Attramadal et al., 1985).

Two Finnish populations of opossum shrimp (*Mysis relicta*) that differ markedly in their susceptibility to light damage (Lindström and Nilsson, 1988) have long been used as research models in the quest for discovering the underlying biochemical and physiological mechanisms. The two populations were separated as the ice shield receded at the end of the latest glaciation (ca. 9000 years ago; Eronen et al., 2001). Their current habitats are a permanently dark and brown, deep freshwater lake and a long narrow bay of the Baltic Sea with variable, but generally brighter, greenish illumination. Consistent with this, the eyes of the lake population have been found to be easily damaged even by moderate light exposures and the recovery of their light responses is slow, whereas those of the Baltic population are more resilient and recover faster (Lindström and Nilsson, 1988; Meyer-Rochow and Lindström, 1997). The populations differ also in spectral sensitivity. This aspect is analyzed in a recent broad overview of relations between spectral sensitivity and photic environment in the *M. relicta* species group (Donner et al., 2016), which includes detailed information on the spectral transmission and absolute light attenuation in the respective habitats. For easy cross-reference, we denote our two present study populations by the same abbreviations as used in that article, L<sub>p</sub> for ‘Lake, Pääjärvi’ and S<sub>p</sub> for ‘Sea, Pojoviken’.

Earlier investigations of the differences in light tolerance have focussed on protective mechanisms and, although some candidates have been identified, the explanatory power has been modest. Dontsov et al. (1999) reported greater amounts of screening pigments, ommochromes, which have antioxidant properties and might thus protect against peroxidation, in the eyes of specimens belonging to the S<sub>p</sub> population. However, Feldman et al. (2008) found that the total antioxidant activity was similar in the eyes of both populations. The concentrations as well as composition of screening pigments vary between L<sub>p</sub> and S<sub>p</sub> (Abu Khamidakh et al., 2010), but optical screening preventing light from reaching photoreceptors cannot, *per se*, be a useful protective strategy in dark-adapted eyes of animals that need to maximize sensitivity. A later study by Feldman et al. (2010) shifted interest to differences in factors that may sensitize eyes to light damage. L<sub>p</sub> eyes were found to have a significantly higher content of retinoids than do S<sub>p</sub> eyes. The authors suggested that the high concentration of precursors of the chromophore (retinal) may reflect a need for efficient ‘dark’ (re)generation of native visual pigment in the extremely dark and

<sup>1</sup>Department of Biosciences, University of Helsinki, 00014 Helsinki, Finland.

<sup>2</sup>School of Life Sciences, University of Sussex, Brighton BN1 9HR, UK. <sup>3</sup>Tvärminne Zoological Station, University of Helsinki, 10900 Hanko, Finland.

\*Author for correspondence (martta.viljanen@helsinki.fi)

 M.L.M.V., 0000-0001-7363-6729

**List of symbols and abbreviations**

A1	retinal
A2	3,4-didehydroretinal
EM	electron microscopy
ERG	electroretinography
$I$	stimulus intensity
$I_{1/2}$	stimulus intensity eliciting half the saturating response amplitude
IR	infrared
$L_p$	<i>Mysis relicta</i> population of Lake Pääjärvi
MII	metarhodopsin II
MSP	microspectrophotometry
$n$	Naka–Rushton steepness coefficient
R	rhodopsin
S	sensitivity
$S_p$	<i>Mysis relicta</i> population of Pojoviken Bay (Baltic Sea)
TEM	transmission electron microscopy
$U$	response amplitude
$U_{max}$	amplitude of saturating light response
$\lambda_{max}$	wavelength of maximal absorption/transmission/sensitivity

reddish lake environment, where photoreconversion of metarhodopsin II (MII) back to native rhodopsin (R) by shorter-wavelength light cannot occur (cf. Donner et al., 1994). The latter mechanism is generally thought to dominate regeneration in bistable arthropod pigments, establishing illumination-dependent R:MII equilibria (e.g. Stavenga and Hardie, 2011). Feldman et al. (2010) argued that this might work in  $S_p$ , whereas  $L_p$  animals in their very dark habitat can only rely on ‘dark’ regeneration. This would keep microvillar membranes constantly loaded with high concentrations of native R liable to trigger massive and damaging photoactivation if the eyes are suddenly exposed to brighter light.

The purpose of the experiments reported here was to test the two-pronged hypothesis that the susceptibility to light-induced damage (1) correlates with the concentration of native rhodopsin in the rhabdomeric membranes, and (2) can (thus) be alleviated by ultra-slow acclimation to red background light, increased in intensity so slowly as not to cause light damage in itself. Obviously, sub-hypothesis 2 is more comprehensive than 1 because it encompasses all physiological changes that may be triggered by slow acclimation, not only the conversion of native R to MII. In an attempt to test the possible importance of the R:MII equilibrium as such, we further examined whether vulnerability could be affected by subsequent blue-light acclimation, presumed to shift the equilibrium back towards R.

**MATERIALS AND METHODS****Study animals**

Adult specimens of the opossum shrimp *Mysis relicta* Lovén 1862 s. str. from two different populations ( $L_p$  and  $S_p$ ; see above) were used for the experiments. The species is a small aquatic crustacean with prominent eyes (Fig. 1A) and a typical diel vertical migration pattern correlated to illumination levels (Beeton and Bowers, 1982). The general structure of the eye closely resembles that of *Praunus flexuosus* described by Hallberg (1977). It is a refracting superposition eye, well adapted to life in environments where light is scarce, as the clear zone between the dioptric apparatus and photoreceptor layer (Fig. 1B) allows each rhabdom to receive light from several ommatidia. The amount of light impinging on the photoreceptors is regulated by screening pigments between and within ommatidia, positioned dependent on the general illumination level.

The  $L_p$  animals were captured with a vertical net from an 80 m deep abyss and the  $S_p$  animals by a sledge net from about 20 m depth, both in May. To avoid photodamage, all animals were shielded as well as possible during capture and afterwards, and the  $L_p$  animals were collected in the night. The animals from both populations were transferred to Tvärminne Zoological Station in light-tight cool boxes. They were housed there in two light-tight cabinets at 7–9°C in aquaria with flow-through brackish water supply and fed fish flakes once a week. All handling of the animals was carried out in infrared (IR) light using IR viewers.

**Experimental setup**

One of the two cabinets holding the aquaria was kept dark all the time, whereas the other one had an inbuilt LED system for adjusting the acclimation lights (Fig. 2A). Three different acclimation protocols (referred to as ‘treatments’) were applied. In treatment I, animals were kept in complete darkness for 1–2 months. In treatment II, a daily 12 h:12 h light:dark cycle of stepwise-increasing dim red background light ( $\lambda_{max}=630$  nm) was introduced in order to promote the conversion of R to MII. The intensity of the red light was increased from zero up to a final value of  $4.4 \times 10^{12}$  photons  $\text{cm}^{-2} \text{s}^{-1}$  in daily steps over either 4 or 2 weeks (‘slow’ and ‘fast’ acclimation; see below). Before the light acclimation was started, the animals were housed for at least 1 month in darkness to allow recovery from light exposures during capture and transfer. In treatment III, blue background light ( $\lambda_{max}=465$  nm) was added on top of the red background after completion of the rising red ramp; this was also increased in small steps from zero up to a total flux (red+blue) of  $6.9 \times 10^{12}$  photons  $\text{cm}^{-2} \text{s}^{-1}$ . Two full acclimation experiments were

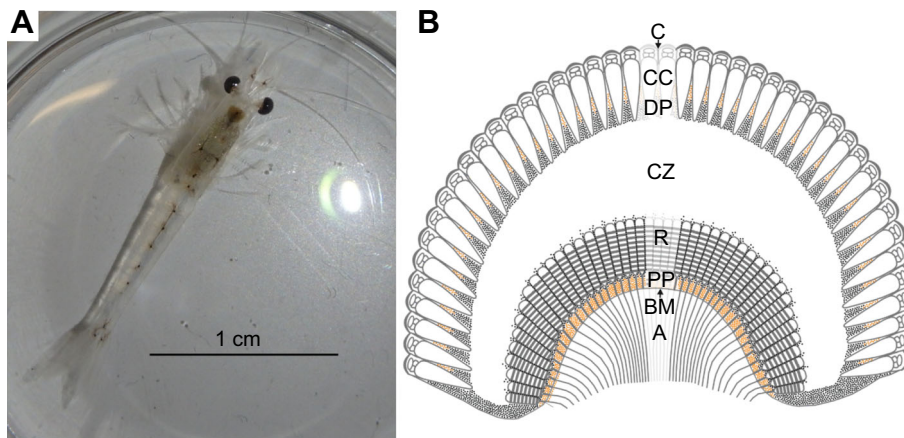


**Fig. 1. *Mysis relicta* and its eye.** (A) Adult *M. relicta*. Note the large and prominent eyes. (B) Schematic diagram of the refractive superposition eye with screening pigments as seen in the preparations. Two kinds of screening pigments, orange and dark, can be seen in both the proximal and distal region of the ommatidia. The screening pigments are mainly located between cells, but the dark proximal pigment granules are found inside photoreceptor cells. C, cornea; CC, crystalline cone; DP, distal screening pigments; CZ, optically clear zone containing the visual cell somas; R, rhabdomeric layer; PP, proximal screening pigments; BM, basal membrane; A, photoreceptor axons.

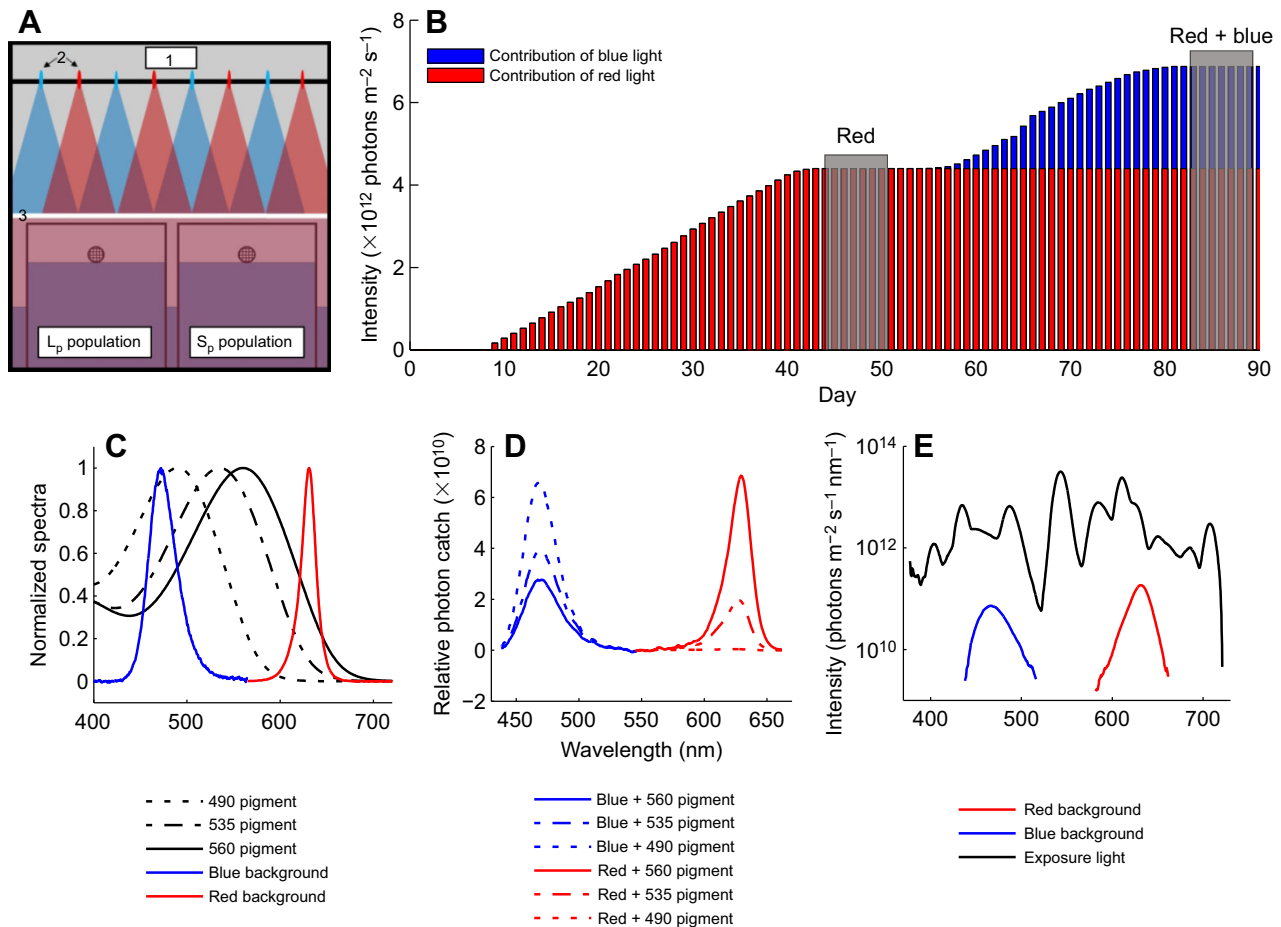


**Fig. 2. Experimental setup for light acclimations.** (A) Schematic diagram of housing conditions: (1) LED controller, (2) blue and red LEDs, (3) diffuser. The intensities of the red and blue LEDs are adjusted independently and stepwise during the acclimation period. The whole setup is located in a light-tight cabinet. There is a continuous flow of brackish water; excess water flows out through holes covered with net dense enough to prevent the animals from escaping.  $L_p$ , lake, Pääjärvi;  $S_p$ , sea, Pojoviken. (B) Protocol for slow light acclimation: stepping up of light intensity as a function of time (abscissa, days). Red and blue bars give the intensities of the red and blue LEDs, respectively. Grey shaded zones marked 'Red' and 'Red+blue' indicate the periods during which samples were taken and studied by microspectrophotometry, electron microscopy and electroretinography. (C) Normalized spectra of the red and blue LEDs used for light acclimation, and Govardovskii et al. (2000) templates for 3,4-didehydroretinal (A2) visual pigments with  $\lambda_{max}$  at 560 (solid curve,  $L_p$  pigment), 535 (dashed curve,  $S_p$  pigment) and 490 nm [dotted curve representing metarhodopsin II (MII)]. A2 templates were used, in line with previous studies, because they provide good single-parameter phenomenological descriptions of the empirical data, even though the study populations only have A1 (see Donner et al., 2016). The red LED spectrum overlaps with the spectra of the native rhodopsins (R), but not with that of MII. The blue LED spectrum overlaps with all of the pigment spectra, but most strongly with that of MII. Thus, the red background illumination is expected only to convert R to MII but not *vice versa*, and the blue illumination to cause more reconversion (as fractions of the amounts present) of MII to R than the other way round. (D) Relative photon-catch spectra for the different visual pigments from the acclimating lights (blue and red curves): R(560), solid lines; R(535), dashed lines; MII(490), dotted lines. The total photon catch in each case is the integral of the spectrum (area under the curve). Absorption of the red acclimating light is considerably higher in R(560) than in R(535) and negligible in MII, whereas absorption of the blue acclimating light in R(560) is almost equal to that of the red light and much higher in R(535) and especially in MII. When both lights are on at their maximal level, absorption in MII exceeds that in either of the native pigments. (E) Top curve (black): absolute photon flux spectrum of the bright 'white' exposure light. Bottom curves: the spectra of the red and blue acclimating lights at their maximal levels shown for comparison. Note logarithmic ordinate.

run (in different years) that were identical other than that the time of ramping-up of the acclimation lights differed by 2-fold, so that the total duration of the experiment was either 3 months ('slow' acclimation, as schematically shown in Fig. 2B) or half that time ('fast' acclimation).

The absolute irradiance spectra of the lights for acclimation and bright-light exposures [as well as the stimulus lights used in the electroretinography (ERG) experiments; see further below] were measured with an OceanOptics JAZ spectrometer with optic fibre and cosine corrector, and the obtained spectra were further processed in Matlab. Relative photon catches from the acclimating lights were estimated by convolution of the emission spectra of the respective LEDs with visual-pigment templates (Govardovskii

et al., 2000) for  $\lambda_{max}$ =490 nm (representing MII), 535 nm (for native  $S_p$ ) and 560 nm (for native  $L_p$ ) (Jokela-Määttä et al., 2005; Donner et al., 2016). In line with the earlier studies, 3,4-didehydroretinal (A2) templates were used because they provide a convenient single-parameter phenomenological description of spectra recorded from single rhabdoms (Jokela-Määttä et al., 2005; Donner et al., 2016), even though the study populations have been shown to utilize only retinal (A1) (Belikov et al., 2014). The likely reason for this is that whole-rhabdom absorption spectra of both  $S_p$  and  $L_p$  are broadened by a minor component contributed by the pigment that is dominant in the other population (see Donner et al., 2016). The LED emission spectra, visual-pigment templates and resulting photon-catch spectra are shown in Fig. 2C,D.

Samples of animals were taken from the acclimation aquaria at two time points: after completion of the red ramp and after completion of the blue ramp (time intervals Red and Red + blue in Fig. 2B). At the first sampling point, ‘dark’ samples were also taken from the dark cabinet. Half of the animals from each sample were subsequently kept in total darkness (‘controls’), whereas the other half (‘exposed’) were subjected to a 15–30 min exposure of bright white light (intensity  $1.4 \times 10^{15}$  photons  $\text{m}^{-2} \text{s}^{-1}$ ). The spectrum of the exposure light is shown in Fig. 2E together with the spectra of the acclimation lights at their maximal levels (note logarithmic ordinate). The eyes and rhabdoms of all samples were investigated by three methods: whole-eye ERG to measure light responsiveness, single-rhabdom microspectrophotometry (MSP) to measure visual-pigment content and transmission electron microscopy (TEM) to measure the integrity of the microvillar organization of the photoreceptor cells. All experiments were carried out during the daytime, and the exact experimental times can be found in Table S1.

### ERG

All preparations were done in darkness using only IR illumination and IR converter. Control animals were decapitated immediately after they were brought to the laboratory and ‘exposed’ animals only after the exposure to bright white light (see above). One eye of each animal was put aside for preparation of TEM samples and the other eye was prepared for ERG as described by Lindström and Nilsson (1983, 1988) and Jokela-Määttä et al. (2005). Preparation lasted 10–15 min, after which the eye was left to rest in darkness for 30–40 min. The specimens were kept moist at 9°C.

A Narva 6 V 15 W (no. 26.1649/06) light bulb with a stabilized power supply was used as stimulus light source with intensity adjusted by neutral density (ND) filters and wedge inserted in the beam. The light from the lamp measured at the level of the preparation (photons  $\text{nm}^{-1} \text{cm}^{-2} \text{s}^{-1}$ ) was translated into conceptual ‘Mysis-relevant intensities’ (Mysis-photons  $\text{cm}^{-2} \text{s}^{-1}$ ) by convolution with the Govardovskii et al. (2000) A2 template for  $\lambda_{\text{max}}=545$  nm, which represents the empirical mean for the two study populations. As such, this has no deeper physiological significance here, because we do not estimate actual rates of photoisomerizations, but was done in order not to report misleadingly high photon fluxes due to the dominance of very long wavelengths in the emission spectrum of the light bulb.

Response families were recorded with 500 ms pulses of light in increasing intensity order given at 1–2 min intervals. Response amplitudes ( $\mu\text{V}$ ) were plotted as functions of pulse intensity (Mysis-photons  $\text{cm}^{-2}$ ) and the intensity–response ( $I$ – $R$ ) functions were fitted with the Naka–Rushton modification of the Michaelis–Menten function:

$$U/U_{\text{max}} = I^n / (I^n + I_{1/2}^n), \quad (1)$$

where  $U$  is response amplitude and  $I$  is stimulus intensity; the parameters are the amplitude of saturated responses ( $U_{\text{max}}$ ), the ‘half-saturating’ stimulus intensity ( $I_{1/2}$ ; i.e. that which elicits a response of amplitude  $0.5 U_{\text{max}}$ ) and a steepness parameter ( $n$ ). Although truly saturated responses could generally not be recorded owing to the limitation of the light source, fitting Eqn. (1) to the data allowed reasonably accurate determination of the two most crucial characteristics of eye responsiveness: sensitivity, defined as  $S=1/I_{1/2}$  and the maximal response amplitude,  $U_{\text{max}}$ . The best fit was found by iteration in Matlab. When fitting, the three parameters are not independent, but the minor variation in  $n$  that was allowed would not significantly affect the estimates of  $I_{1/2}$  and  $U_{\text{max}}$ .

For the dark-adapted animals, it was possible to pool the data from both series of acclimation experiments (fast and slow) to increase the number of observations because they had been through the same treatment in both cases. Differences in  $U_{\text{max}}$  between treatments were tested by Student’s  $t$ -test on log-transformed values because the light intensity settings are logarithmically spaced. The main hypotheses were one-sided: firstly, that bright-light exposure depresses  $U_{\text{max}}$  and decreases  $S$  in all conditions; secondly, that  $U_{\text{max}}$  and  $S$  after bright-light exposure are higher in animals that have undergone light acclimation than in animals acclimated to darkness. Thus, these were statistically assessed by one-tailed probabilities. In other cases, two-tailed probabilities applied.

### Histology for TEM

A procedure modified from Nilsson (1982) was applied to the samples prepared for TEM. Eyes were prefixed at Tvärminne Zoological Station, Finland in modified Karnovsky solution (5% glutaraldehyde and 4% paraformaldehyde in  $0.2 \text{ mol l}^{-1}$  cacodylate buffer) for 3 h and stored in  $0.1 \text{ mol l}^{-1}$  cacodylate buffer with 2% paraformaldehyde for 1–20 days, before postfixation at the Electron Microscopy Unit of the Institute of Biotechnology at the University of Helsinki, Finland. Postfixation was carried out in  $0.2 \text{ mol l}^{-1}$  cacodylate buffer with 2%  $\text{OsO}_4$  for 2 h at 4°C, after which the samples were dehydrated and embedded in epoxy resin. Ultrathin sections were made and observed using a JEM1011 electron microscope. TEM micrographs were taken of samples from one or two control and experimental animals for each treatment using an Orius CCD camera SC200 (Gatan) and DigitalMicrograph software.

Fig. 3 shows examples of EM micrographs of rhabdoms with different levels of morphological order/disorder. The degree of disorder was quantified on a five-score ordinal scale, where 0 means that microvilli are practically perfectly organized (Fig. 3A) and 4 that organization is almost completely lost (Fig. 3C). This was done at multiple sites in each sample and, when possible, at different sites along the rhabdom. A major challenge in quantifying structural changes was that they were not uniform over the eye, but varied strongly from site to site. Because it was not possible to map whole rhabdoms and perform proper statistics, we therefore report values based on the best and the worst sites of each specimen (see below).

### MSP

Absorption spectra of single rhabdoms were recorded with a single-beam, fast wavelength-scanning microspectrophotometer (Govardovskii et al., 2000) in samples of three control and three exposed animals from both populations ( $L_p$  and  $S_p$ ) from each ‘slow’ acclimation treatment. The MSP was carried out in Helsinki, where the animals were transferred from Tvärminne alive in light-tight containers 1–2 days before measurements. The bright-light exposures were done exactly as for the ERG experiments (see above), after which the animals were left to dark adapt for 3–8 h before measurements. Preparations were made at room temperature under IR light in crayfish saline ( $0.2 \text{ mol l}^{-1}$  NaCl;  $5.4 \text{ mmol l}^{-1}$  KCl;  $13.6 \text{ mmol l}^{-1}$   $\text{CaCl}_2$ ;  $2.6 \text{ mmol l}^{-1}$   $\text{MgCl}_2 \cdot 6\text{H}_2\text{O}$  and  $5 \text{ mmol l}^{-1}$  Hepes; pH 7.6). The animals were decapitated and the rhabdom layer was separated from the rest of the eye in a drop of saline, placed between two cover-glasses sealed with grease and gently squeezed to slightly flatten the rhabdoms. Absorption spectra were recorded from 10–30 rhabdoms per animal but, owing to quality problems, only 1–13 per animal were included in the analyses. In particular, rhabdoms of the animals that had been exposed to bright light were generally in a bad condition and covered with dark screening pigment. Avoiding artefacts due to screening pigments

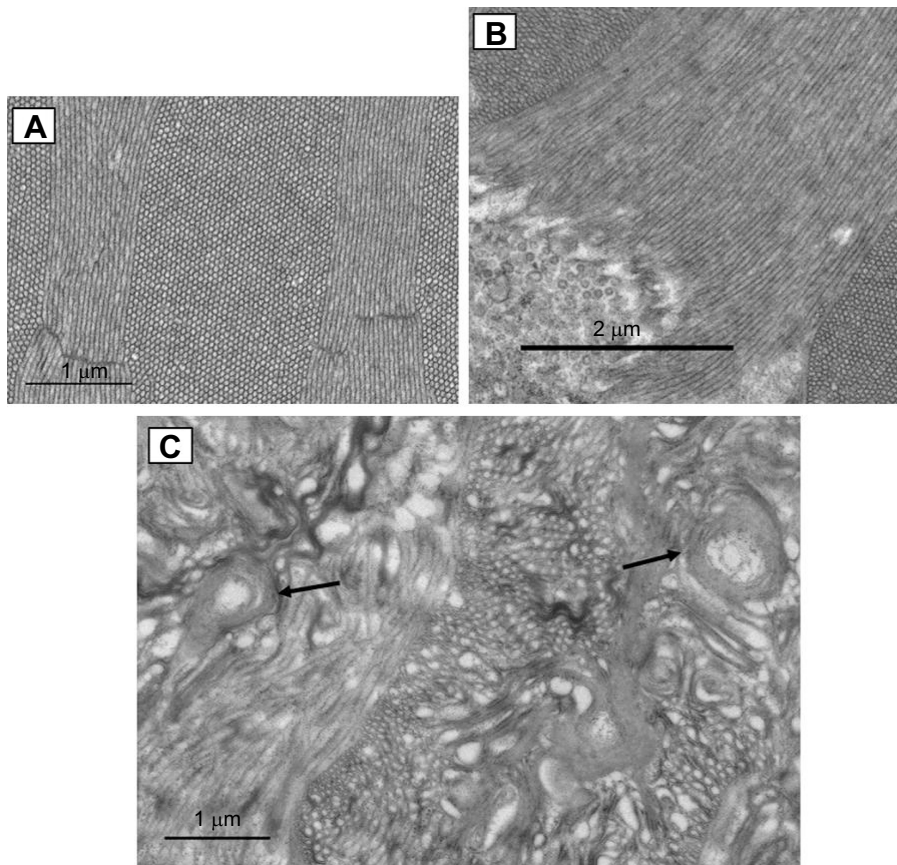


**Fig. 3. Structure, arrangement and disorder score of rhabdomal microvilli as seen in electron micrographs.** (A) Score 0 of morphological (dis)order. The arrangement of the microvilli is completely regular and there are no signs of swollen microvilli or whorl formations. (B) 'Pinching': vesicles at the base of rhabdomal microvilli resembling the coated vesicles reported to be part of classical renewal of the microvilli. (C) Score 4 of morphological disorder: the regularity of the microvillar arrangement is almost completely lost and there are lots of fused microvilli. Whorls typical of microvillar damage are marked with arrows.

sometimes entailed excluding most of the recorded spectra from further analysis. Spectra were processed and the wavelength of maximal absorbance ( $\lambda_{\max}$ ) for each animal was determined as described by Govardovskii et al. (2000). To test the photoactivity of the pigment, some rhabdoms were exposed to strong 550 nm light delivered for 2 min through the measuring beam, and the difference between pre- and post-exposure spectra was observed.

## RESULTS

### Changes in single-rhabdom absorption spectra after slow light acclimation

The light acclimation treatments changed the absorption spectra of single rhabdoms as exemplified in Fig. 4 by recordings from

individual  $L_p$  animals. In both populations, the main absorption peak tended to decrease, indicating photoconversion ('bleaching') of native rhodopsin. The decrease occurred throughout both the first (red) and the second (red+blue) acclimation epoch, indicating that (contrary to our intentions) no net reconversion of MII to R was achieved by adding the blue light. In  $L_p$  rhabdoms, the first acclimation epoch brought little or no change in  $\lambda_{\max}$  (middle versus leftmost panel in Fig. 4), implying that absorption by native  $L_p$  pigment (~560 nm) remained completely dominant. During the second acclimation epoch, however, the spectrum moved towards shorter wavelengths (rightmost panel in Fig. 4). This indicates a further decrease in native  $L_p$  pigment and is consistent with a shift of the R:MII balance towards MII (~490 nm) (see further below, however).

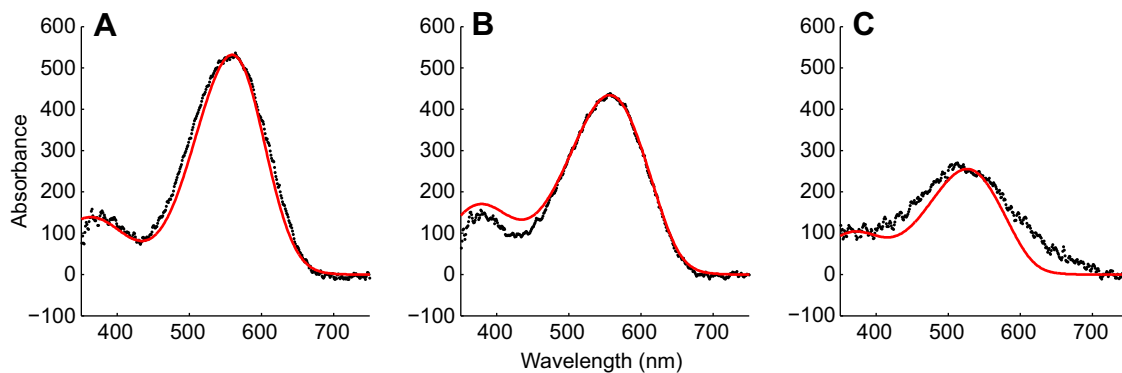


**Fig. 4. Single-rhabdom absorption spectra.** Single-rhabdom absorption spectra of individual  $L_p$  control animals under dark acclimation (A), after slow red light acclimation (B) and after slow red+blue light acclimation (C). Black dots represent averaged measurements from 6–10 rhabdoms of an individual animal and the red line an A2 template fitted to the data. Note the consistent decrease in peak absorbance, indicating decreasing native pigment density, and the shift of the rightmost spectrum towards shorter wavelengths, presumably reflecting photoconversion of R to MII.

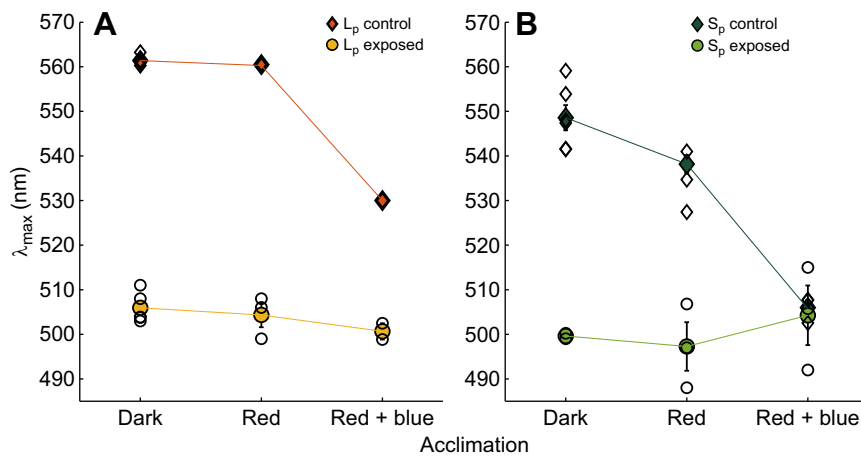


**Fig. 5.  $\lambda_{\max}$  values of rhabdoms under the slow acclimation protocol.** Means  $\pm$  s.e.m. are shown; top curve: control animals; bottom curve: bright-light-exposed animals.  $\lambda_{\max}$  of individual animals are marked with open symbols. (A)  $L_p$  population results. The  $\lambda_{\max}$  of control animals shifted to shorter wavelengths during light acclimation, suggesting a shift of the R:MII equilibrium towards MII, whereas the  $\lambda_{\max}$  of bright-light-exposed animals was virtually constant. However,  $\lambda_{\max}$  of exposed animals was always at longer wavelengths than that of MII (490 nm), indicating the presence of some native R. Numbers of animals in different acclimations (control/exposed): dark  $N=5/N=5$ , red  $N=3/N=3$ , red+blue  $N=1/N=2$ . (B) Same as A, but for  $S_p$  animals. Numbers of animals in different acclimations (control/exposed): dark  $N=6/N=2$ , red  $N=3/N=3$ , red+blue  $N=3/N=3$ .

Fig. 5A,B summarizes the MSP data for rhabdoms of both populations in terms of  $\lambda_{\max}$  in each condition. The original mean values ('dark') were 561 nm for  $L_p$  and 549 for  $S_p$ . The first epoch of slow acclimation to red light left the mean  $\lambda_{\max}$  virtually unchanged in  $L_p$ . In  $S_p$ , however, mean  $\lambda_{\max}$  dropped to 535 nm, which, admittedly, may be at least partly attributed to selective bleaching of the small proportion of  $L_p$  pigment present, thus increasing the dominance of the  $S_p$  majority pigment (see Zak et al., 2013; Donner et al., 2016). After the second acclimation epoch (red+blue), the mean  $\lambda_{\max}$  values of both populations had decreased significantly, to 530 nm in  $L_p$  and 506 nm in  $S_p$ . At least the latter value is lower than any native *M. relictus* pigment and must to a significant extent be due to MII absorbance. Inter-individual variation was small in  $L_p$ , whereas, in  $S_p$ , there was considerable dispersion of individual  $\lambda_{\max}$  values. This large variation within  $S_p$  and the fact that the mean dark-adapted  $\lambda_{\max}$  was much higher than values reported earlier for that population (Jokela-Määttä et al., 2005; Donner et al., 2016) suggest that the present  $S_p$  sample had unusually high and variable proportions of the minority pigment (Donner et al., 2016).

Some rhabdoms of control animals from all acclimation treatments were exposed to strong light through the microspectrophotometer (see Materials and methods). The large differences between pre- and post-bleach spectra confirmed that the pigments underlying the main absorption bands were photoactive also in isolated rhabdoms of  $L_p$  controls, where the end point after red+blue acclimation suggested less complete photoconversion of native pigment than in  $S_p$ . By contrast, the absorption spectra of rhabdoms isolated from animals that had (before decapitation) been exposed to bright light as part of the experimental protocol (bottom curves in Fig. 5A,B) were not significantly affected by further bright-light exposures. The main conclusion from the MSP is that our light acclimation protocols did shift the R:MII ratio towards MII as intended, although the initial decrease of  $\lambda_{\max}$  especially in  $S_p$  may be due partly to selective bleaching of the longer-wavelength (~560 nm) native visual pigment (Zak et al., 2013; Donner et al., 2016). However, reconversion of MII to R by the addition of blue light could not be clearly observed, unless the apparently higher final R:MII ratio in  $L_p$  than in  $S_p$  controls be interpreted in this way.

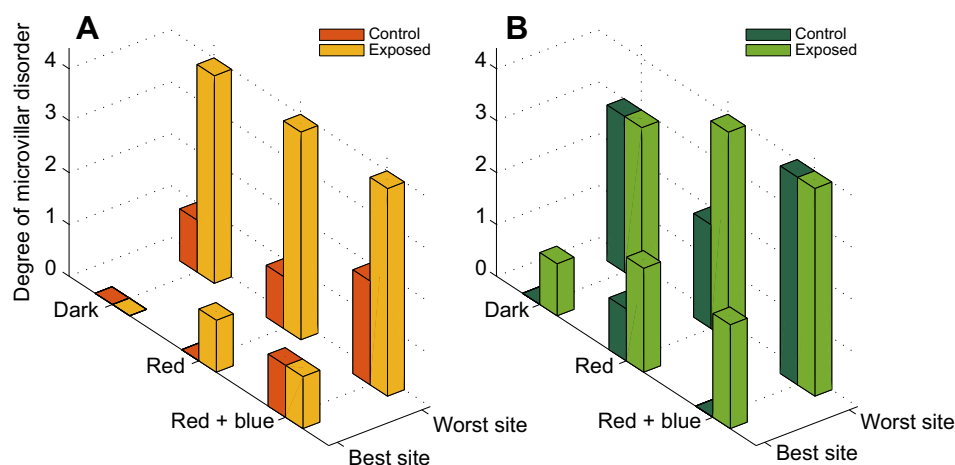


**Fig. 6. Range of microvillar disorganization found in rhabdoms under the slow acclimation protocols, measured on a qualitative ordinal scale from 0 to 4.** The value 0 means that microvillar organization is completely regular and the value 4 that it is almost completely lost (see Fig. 3). (A)  $L_p$  results. Red bars refer to control animals, yellow bars to animals that have been exposed to bright light. The front row gives the measures for the best sites found and the back row for the worst sites found. Bright-light exposure can be seen to cause disorganization in all conditions, but organization is impaired to some extent and in a graded manner by the light acclimation itself, so that the scores for control animals are dark < red < red+blue. Note, however, that the best and worst sites differ to some extent even in rhabdoms of completely dark-adapted controls, indicating that even these are not homogeneously well organized. (B) Same as A, but for  $S_p$  rhabdoms. The microvilli of control animals are more organized than those of exposed animals in all conditions, but the general effect of the light acclimations are not clear. Note again the difference between the best and worst sites even in dark-adapted controls.

The net changes during the red+blue acclimation epoch went in the same direction as under pure-red-light acclimation.

### Microvillar ultrastructure

Owing to the small number of EM samples, the results can be only qualitative and suggestive. As explained in the Materials and Methods, a number of sites in each sample were scored on an ordinal scale for microvillar disorganization from 0 to 4. The worst sites showed membrane whorl formations typical of damage caused by light or some other factor (score 4, see Fig. 3C). Score 0 refers to near-perfect regularity (Fig. 3A). In many fairly well-ordered samples, though, there were vesicles to be seen at the base of microvilli, commonly associated with membrane cycling in arthropods (see Fig. 3B).

### Slow acclimation

The disorganization scores of the best and worst sites observed in control and exposed samples under the slow acclimation protocol are summarized in Fig. 6 for both  $L_p$  (panel A) and  $S_p$  (panel B). The observations did not really conform to our expectations, save for the most basic fact that the bright-light exposures invariably compromised microvillar organization as judged either by the best or the worst site, or both. However, there was no indication that  $L_p$  rhabdoms are structurally more easily disorganized by bright-light exposures than  $S_p$  rhabdoms. The best sites in dark-acclimated  $L_p$  rhabdoms remained fairly well ordered after exposure and, in all cases, better than in  $S_p$  animals. Secondly, there was no indication that slow light acclimation could mitigate structural damage from bright-light exposures. The worst sites of exposed animals from both populations scored 4 (maximal disorder) after both red and red+blue acclimation. In contrast, the differences between the best and the worst sites even in dark-acclimated controls of both populations indicate that variation in microvillar organization within rhabdoms is not necessarily dependent on light exposures, but part of normal membrane dynamics. The greater disorganization in  $S_p$  animals may indicate faster membrane cycling overall. On the whole, there was a lot of variation in the degree of microvillar disorder within samples, some samples covering the whole scale from 0 to 4.

### Fast acclimation

In the samples from animals that had been subjected to the fast acclimation protocol, only the best sites were ranked because the light acclimation in itself caused significant microvillar disarrangement. All best sites of light-acclimated controls scored 2 in both populations, save for  $S_p$  after red+blue acclimation, which

scored 1 (results not shown). Instead, subsequent bright-light exposures did not exacerbate disorder in any of the cases. The disruptive effects of the 2-week red illumination ramp compared with the absence of any systematic degradation due to the 4-week ramp (cf. controls in Fig. 6) may serve to calibrate the capacity of the physiological acclimation mechanisms to cope with gradients of general illumination change (see Discussion).

Yet, our sparse EM sampling can provide only a coarse picture. A firm answer to the question of to what extent slow light acclimation can protect the structural integrity of microvillar organization would require more comprehensive statistical quantification of the state of entire rhabdoms.

### Changes in light responsiveness of whole eyes measured by ERG

The ERG field potential gives a gross measure of the functional integrity of the whole eye, averaged across rhabdoms, rhabdomeres and sites that have suffered various degrees of damage. The effects can be assessed from changes in the  $I$ - $R$  function (response amplitude plotted as a function of the intensity of the light stimuli). Eqn (1) provides a phenomenological description of the  $I$ - $R$  function with two main parameters: the half-saturating intensity ( $I_{1/2}$ ) and the amplitude of saturated responses ( $U_{max}$ ). The third (steepness) parameter,  $n$ , cannot be given any equally tangible interpretation, nor is it usually necessary to. Fig. 7 shows  $I$ - $R$  data from two individuals, one dark-adapted control and one exposed, fitted with Eqn (1) and displayed both on lin-log (Fig. 7A) and log-log (Fig. 7B) scales. The lin-log presentation makes evident the sheer magnitude of the depression following bright-light exposure. In the log-log presentation it is easier to make a quantitative comparison between the  $I$ - $R$  functions, decreases in  $U_{max}$  appearing as downward shifts and increases in  $I_{1/2}$  as rightward shifts. Because of the limitations of our light source, recordings from bright-light-exposed animals could be obtained only from the lowest part of the function, yet  $U_{max}$  and  $I_{1/2}$  could be determined with reasonable accuracy by curve-fitting.

### Slow acclimation

Figs 8A–D and 9A–D summarize changes in  $U_{max}$  and  $I_{1/2}$  across conditions under the slow acclimation protocol. The saturated response amplitude,  $U_{max}$ , of dark-adapted control animals was somewhat higher in  $L_p$  than in  $S_p$  on average, and this difference between  $L_p$  and  $S_p$  controls persisted throughout acclimations.

The most important result of the present work, directly related to hypothesis 2, is that shown for  $L_p$  in Fig. 8A. Whereas  $U_{max}$  in the

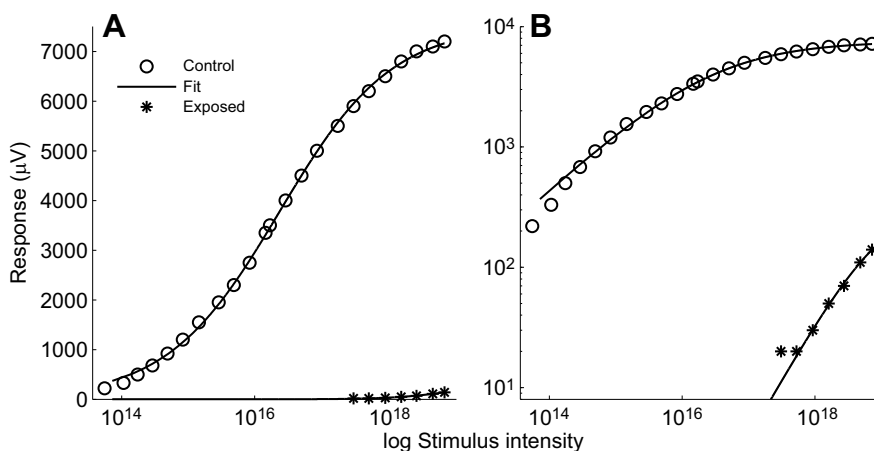


**Fig. 7. Electroretinography intensity–response functions in  $L_p$  animals.** Values were recorded from two individual  $L_p$  animals (one control and one exposed) and fitted with Naka–Rushton functions. (A) Data in traditional sigmoidal lin–log form. (B) Data in log–log form to facilitate assessment of especially the data from exposed animals. The parameters of the functions are: amplitude of saturating light response ( $U_{max}$ )=7545  $\mu$ V, stimulus intensity eliciting half the saturating response amplitude ( $I_{1/2}$ )= $6.3 \times 10^{15}$  photons  $m^{-2} s^{-1}$  and steepness parameter ( $n$ )=0.51 for the control animal, and  $U_{max}$ =351  $\mu$ V,  $I_{1/2}$ = $7.4 \times 10^{17}$  photons  $m^{-2} s^{-1}$  and  $n$ =0.97 for the exposed animal.

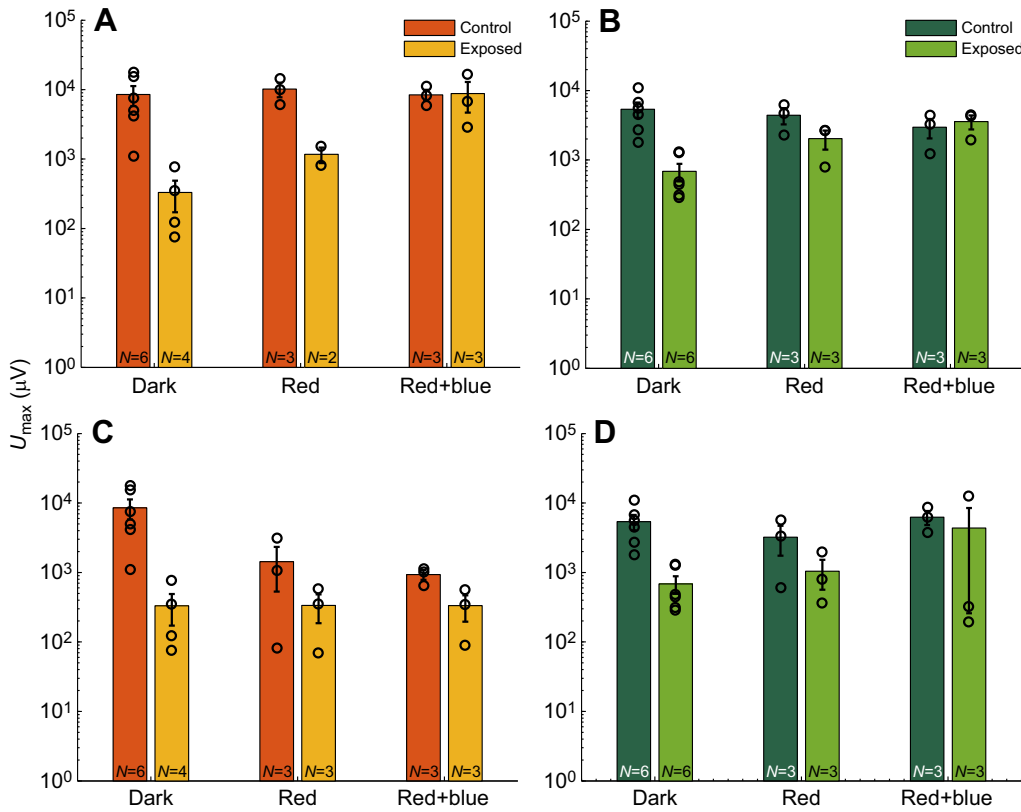


**Fig. 8. Saturated response amplitudes under the slow (top panels) and fast (bottom panels) acclimation protocols.** Dark acclimation represents combined results of both protocols [3 animals/protocol, except 1 exposed  $L_p$  animal in the fast acclimation]. Results from individual animals are marked with open circles. (A)  $U_{max}$  of  $L_p$  eyes (means $\pm$ s.e.m.) under the slow acclimation. (B) Same as A, but for  $S_p$  eyes. (C)  $U_{max}$  of  $L_p$  eyes (means $\pm$ s.e.m.) under the fast acclimation. (D) Same as C but for  $S_p$  eyes.

eyes of dark-acclimated animals that had been subjected to the standard bright-light exposure were, on average, depressed by 20- to 30-fold compared with unexposed controls from the same group, after the red-light-acclimation epoch, the  $U_{max}$  depression of exposed animals was only  $\sim$ 10-fold compared with controls and,

after the second (red+blue) acclimation epoch,  $U_{max}$  of the exposed animals was equal to that of controls (and equal to the dark-adapted value at the beginning of the experiment). In statistical terms, control  $U_{max}$  was larger than exposed  $U_{max}$  in dark-acclimated animals ( $t_8=4.96$ ,  $P=0.0006$ ) and in red-acclimated

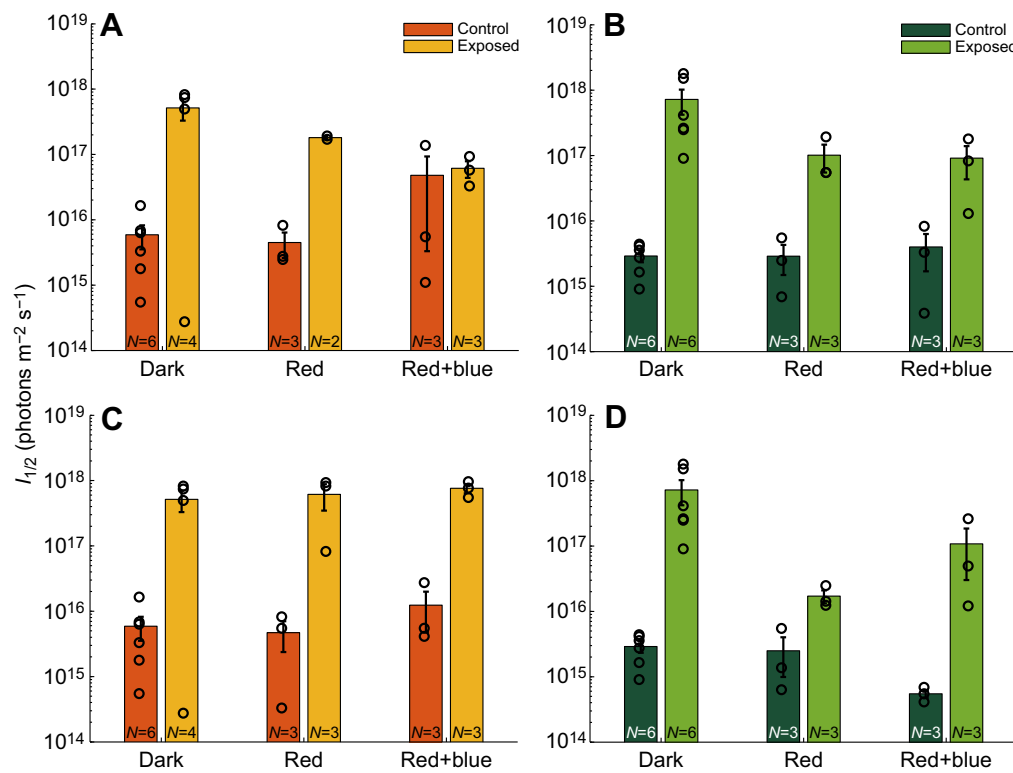


**Fig. 9. Stimulus intensity eliciting half the saturating response amplitude.** Half-saturating intensities ( $I_{1/2}$ ) under the slow (A,B) and fast (C,D) acclimation protocols (A,C:  $L_p$ ; B,D:  $S_p$ ). Dark acclimation represents combined results of both protocols [3 animals/protocol, except 1 exposed  $L_p$  animal in the fast acclimation]. Results from individual animals are marked with open circles. (A)  $I_{1/2}$  (photons  $m^{-2} s^{-1}$ ) of  $L_p$  eyes (means $\pm$ s.e.m.) under the slow acclimation. (B) Same as A but for  $S_p$  eyes. (C)  $I_{1/2}$  (photons  $m^{-2} s^{-1}$ ) of  $L_p$  eyes (means $\pm$ s.e.m.) under the fast acclimation. (D) Same as C but for  $S_p$  eyes.



( $t_3=5.37$ ,  $P=0.006$ ), whereas, in red+blue-acclimated animals, there was no significant difference. Comparing the exposed groups,  $U_{\max}$  of red+blue-acclimated animals was statistically significantly higher than that of dark-acclimated animals ( $t_5=4.57$ ,  $P=0.003$ ) and the same was (nearly) true of red-acclimated compared with dark-acclimated animals ( $t_4=1.99$ ,  $P=0.06$ ).

The saturated responses of control  $L_p$  animals remained remarkably constant throughout the slow acclimations.

In  $S_p$  (Fig. 8B), the general pattern was broadly similar, but depressions due to bright-light exposures were smaller than in  $L_p$ , consistent with earlier studies (e.g. Lindström and Nilsson, 1988). In dark-acclimated animals,  $U_{\max}$  of controls was somewhat less than 10-times higher compared with exposed animals ( $t_{10}=5.49$ ,  $P=0.0001$ ). The difference decreased to 2- to 3-fold after the first (red) light acclimation epoch and disappeared under the second (red+blue), both because exposed  $U_{\max}$  grew and control  $U_{\max}$  declined gently. Thus, the slow light acclimations raised the  $U_{\max}$  of bright-light-exposed animals to the level of controls. Comparing the exposed groups,  $U_{\max}$  of both red+blue-acclimated and red-acclimated animals was statistically significantly higher than that of dark-acclimated animals ( $t_7=4.05$ ,  $P=0.002$  and  $t_7=2.38$ ,  $P=0.02$ , respectively).

### Fast acclimation

The time scale of light acclimation had a notable effect on the ERG results (Fig. 8C,D). When the red illumination was ramped up in 2 weeks ('fast') instead of 4 weeks ('slow'), the light acclimation in itself depressed  $U_{\max}$  in  $L_p$  animals compared with dark-acclimated controls ( $t_7=2.39$ ,  $P=0.05$ ) and the trend continued during the red+blue epoch ( $t_7=3.06$ ,  $P=0.02$ ).  $U_{\max}$  after bright-light exposures remained on the same level under all acclimation treatments (dark, red and red+blue), so fast light acclimations caused neither protection nor extra vulnerability. An alternative way of expressing the same thing would be that the acclimations decreased the differences between control and exposed animals. In  $S_p$  animals, by contrast, control  $U_{\max}$  changed little, and there was a suggestion, although not statistically significant, that the effects of subsequent bright-light exposures may have been somewhat mitigated even by the fast acclimation protocol.

The half-saturating intensity  $I_{1/2}$  (Fig. 9) is an inverse measure of 'fractional' sensitivity, i.e. the fraction of the maximal response amplitude that is elicited by one photoisomerization. Bearing this in mind, the changes in  $I_{1/2}$  broadly paralleled those of  $U_{\max}$  (i.e. decreases in  $U_{\max}$  correlated with increases in  $I_{1/2}$ ). Possible discrepancies between the effects on  $U_{\max}$  and sensitivity cannot be resolved with certainty in view of the substantial random variation. Although a correlation is not unexpected, it should be noted that this is not a purely trivial result because the two entities are, in principle, independent mathematically as well as physiologically.

## DISCUSSION

### Slow light acclimation reduces detrimental effects of bright-light exposures

The ERG results show that acclimation to very slowly increasing background illumination reduces functional depression from exposure to bright light. Dark-acclimated  $L_p$  animals that had been exposed to bright light gave maximum response amplitudes ( $U_{\max}$ ) that were just a few per cent of those from unexposed controls. After slow red-light acclimation,  $U_{\max}$  of bright-light-exposed animals was ~10% of controls and, after red+blue acclimation, exposed and control animals had the same  $U_{\max}$

(Fig. 8A). Remarkably, both  $U_{\max}$  and  $I_{1/2}$  of controls were virtually unaffected by the exposure to very slowly increasing background illumination in itself, indicating that adaptation mechanisms in the eye have sufficient capacity to deal with light gradients of that steepness (see Fig. 2B). The pattern of changes was essentially similar in  $S_p$  animals, although differences between control and exposed animals were smaller to start with (Fig. 8B).

However, the physiological acclimation develops very slowly. A 2-times steeper light gradient (the fast acclimation protocol) decreased  $U_{\max}$  in  $L_p$  controls by 80% (Fig. 8C) and caused significant morphological disorder. This stands in clear contrast to the virtual absence of detrimental effects of the slow acclimation protocol on either ERG responses or the microvillar organization in control animals. The differing effects of the two provide a calibration of the time scale on which the physiological acclimation mechanisms work: the fast protocol involved two ramps stepped up over 2 weeks each (first the red and on top of that the blue ramp), whereas the slow protocol took twice that time (4+4 weeks) to cover the same intensity changes. The acclimation dynamics defined by these two experiments appear to be roughly consistent with the ecological demands of *M. relicta* vision, especially for the  $L_p$  population. Over shorter time scales, the animals can keep the light levels they experience relatively stable by vertical migration (diel or otherwise). By contrast, seasonal changes, which cannot be avoided by swimming behaviour, act on time scales of several weeks or months.

Our sparse EM sampling of rhabdomal structure could provide no definite answers to the question of whether light acclimation can protect against structural damage. The basic difficulty is the patchiness of the disorganization both longitudinally and transversally. To take a relevant example from another arthropod group, Blest and Day (1977) reported finding totally disordered rhabdomeres next to wholly normal cells in the spider *Dolomedes*. Interpretations are further complicated by the fact that microvillar disorganization should be judged in the general context of dynamic membrane cycling in rhabdoms, ranging from normal renewal to various degrees of photodamage. Differences may be more quantitative than qualitative. In our present data, there was substantial heterogeneity in microvillar organization (differences between best and worst sites) even in rhabdoms from animals that had not been exposed to any light at any stage of the experiments (dark-acclimated controls in Fig. 6), most pronounced in  $S_p$  animals. Although light deprivation has also been shown to cause ultrastructural changes in the eyes of some crustaceans (Bloom and Atwood, 1981), this phenomenon has not been found in the eyes of *M. relicta*.

Differences of  $S_p$  compared with  $L_p$  may be interpreted as adaptations to a brighter and more variable natural light environment:  $S_p$  eyes seem to be inherently more dynamic than  $L_p$  eyes. In  $S_p$ ,  $U_{\max}$  behaved similarly under the slow and fast acclimation protocols (Fig. 8B,D). The structural studies suggested faster cycling of microvillar membranes in  $S_p$  than in  $L_p$ . Faster cycling might be linked to changes in the amount or composition of proximal screening pigments or intrinsic properties of the membrane. Some screening pigments have photoprotective activity (Abu Khamidakh et al., 2010; Insausti et al., 2013) and membrane properties are universally regulated by changing lipid composition (see below). It may further be noted that polyunsaturated fatty acids formed as part of the phototransduction reactions have been shown to enhance excitation in *Drosophila* (Chyb et al., 1999).

## The primary change under light acclimation is a decrease of native visual pigment

The MSP results confirmed that the light acclimations caused decreases in the concentrations of native visual pigment. This could be accompanied by elevated MII content and/or a decline in overall visual-pigment content, both reported to occur in bright light (Stavenga and Hardie, 2011). Decreases in visual-pigment content and/or changes in R:III balance might therefore directly contribute to increased resilience by decreasing the direct challenges from massive phototransduction.

The addition of blue light on top of the red light in the acclimations had a similar effect to the red light alone, and indeed MSP spectra gave no indication of a shift of the R:III equilibrium back towards R. This is understandable for two reasons. First, the red background light was continuously present. Second, from Fig. 2C,D, it is obvious that the blue light also excites both the native pigments (535 and 560 nm) quite significantly. Thus, the essential difference between red and red+blue acclimations was probably in the time and intensity of light exposure rather than the spectral distribution of the acclimating lights.

Although the observations on pigment content are qualitatively consistent with our hypothesis 1, it must be emphasized that the increased tolerance to strong light cannot be directly explained by the decrease in native pigment concentration or the R:III balance in the photoreceptors. It continued to develop long after the R concentration had been substantially reduced, and the fast acclimation protocol in itself depressed responsiveness in  $L_p$  animals even during the second (red+blue) acclimation epoch.

In this perspective, the slow light adaptation described here appears as a parallel to other well-known acclimation responses, serving to align the tolerance range for a given variable with its prevailing variation range under seasonal or other relatively slow and/or long-lasting changes. Mechanisms typically involve several molecular/physiological changes acting on different time scales and levels. Temperature acclimation involves adjustment of the fluidity of cell membranes by changes in lipid composition (fish: Cossins and Prosser, 1978; crabs: Cuculescu et al., 1995) and, on an integrative level, changes in neuromuscular function and metabolism (crayfish: Stephens, 1985; fish: Johnston and Dunn, 1987). Thermal and photic stress has been found to change fatty acid composition and the ultrastructure of photoreceptive membranes in crayfish eyes (Kashiwagi et al., 1997). Under salinity acclimation, reported responses range from changes in epithelial  $\text{Na}^+/\text{K}^+$ -ATPase activity (shrimp: McNamara and Torres, 1999; frog: Wu et al., 2014) to whole-organism effects on development (frog tadpoles: Wu and Kam, 2009). In fact, it appears as remarkable that acclimation of eyes and visual function to variations in light levels on the time scale of seasonal changes has not been reported before.

## Conclusions

The concentrations of native visual pigment in the rhabdoms of two *M. relicta* populations that differ in susceptibility to light damage were reduced by background light that was increased daily in very small steps over several weeks on a 12 h:12 h light:dark cycle. Our hypothesis was that this would reduce vulnerability to strong light by preventing overly massive phototransduction events. Consistent with this, there was dramatic improvement in functional resilience to bright-light exposures especially in the population more susceptible to damage. However, the dynamics of acclimation was not consistent with the original hypothesis, but indicates a novel kind of slow physiological adaptation to long-term changes in ambient light levels.

## Acknowledgements

We thank Mr Filip Granö for setting up the LED system for light acclimation, the Electron Microscopy Unit (Institute of Biotechnology, University of Helsinki) and especially Antti Salminen for technical support with EM samples, and Tvärminne Zoological Station and Lammi Biological Station for helping with acquisition and maintenance of the study animals. M.L.M.V. was a member of the LUOVA Doctoral School in Environmental, Food and Biological Sciences of the University of Helsinki. Special thanks go to all members of the TwinLabs (Ala-Laurila/Donner) at the Department of Biosciences of the University of Helsinki for continuous fruitful discussions.

## Competing interests

The authors declare no competing or financial interests.

## Author contributions

Conceptualization: K.D., M.L.M.V., K.M.W.L.; Methodology: all authors; Formal analysis: M.L.M.V.; Investigation: M.L.M.V., N.E.N., C.L.C.-G.; Resources: K.D., K.M.W.L.; Writing – original draft preparation: M.L.M.V.; Writing–review and editing: K.D., M.L.M.V.; Visualization: M.L.M.V.; Supervision: K.D.; Project administration: K.D.; Funding acquisition: K.D., M.L.M.V.

## Funding

The financial support of The Ella and Georg Ehrnrooth Foundation (Ella ja Georg Ehrnroothin Säätiö) and The Finnish Cultural Foundation (Suomen Kulttuurirahasto) (M.L.M.V.), and The Finnish Society of Sciences and Letters (Suomen Tiedeseura) and The Academy of Finland (Suomen Akatemia) (K.D.) is gratefully acknowledged.

## Supplementary information

Supplementary information available online at <http://jeb.biologists.org/lookup/doi/10.1242/jeb.155101.supplemental>

## References

- Abu Khamidakh, A. E., Demchuk, J. V., Zak, P. P., Lindström, M. and Ostrovsky, M. A. (2010). Shortwave light filtration effect on spectral sensitivity of two shrimp populations of *M. relicta* (Mysida). *Moscow Univ. Biol. Sci. Bull. (Engl. Transl.)* **65**, 51–55.
- Attramadal, Y. G., Fosså, J. H. and Nilsson, H. L. (1985). Changes in behaviour and eye-morphology of *Boreomysis megalops* GO Sars (Crustacea: Mysidacea) following exposure to short periods of artificial and natural daylight. *J. Exp. Mar. Biol. Ecol.* **85**, 135–148.
- Beeton, A. M. and Bowers, J. A. (1982). Vertical migration of *Mysis relicta* Lovén. In *Ecology of Mysidacea* (ed. M. D. Morgan), pp. 53–61. The Netherlands: Springer.
- Belikov, N., Yakovleva, M., Feldman, T., Demina, O., Khodonov, A., Lindström, M. and Ostrovsky, M. (2014). Lake and sea populations of *Mysis relicta* (Crustacea, Mysida) with different visual-pigment absorbance spectra use the same A1 chromophore. *PLoS ONE* **9**, e88107.
- Blest, A. D. and Day, W. A. (1977). The rhabdomere organization of some nocturnal Pisaurid spiders in light and darkness. *Philos. Trans. R. Soc. Lond. B Biol. Sci.* **283**, 3–23.
- Bloom, J. W. and Atwood, H. L. (1981). Reversible ultrastructural changes in the rhabdom of the locust eye are induced by long term light deprivation. *J. Comp. Physiol.* **144**, 357–365.
- Chyb, S., Raghu, P. and Hardie, R. C. (1999). Polyunsaturated fatty acids activate the *Drosophila* light-sensitive channels TRP and TRPL. *Nature* **397**, 255–259.
- Cossins, A. R. and Prosser, C. L. (1978). Evolutionary adaptation of membranes to temperature. *Proc. Natl. Acad. Sci. USA* **75**, 2040–2043.
- Cuculescu, M., Hyde, D. and Bowler, K. (1995). Temperature acclimation of marine crabs: Changes in plasma membrane fluidity and lipid composition. *J. therm. Biol.* **20**, 207–222.
- Donner, K. O., Langer, H., Lindström, M. and Schlecht, P. (1994). Visual pigment, dark adaptation and rhodopsin renewal in the eye of *Pontoporeia affinis* (Crustacea, Amphipoda). *J. Comp. Physiol. A* **174**, 451–459.
- Donner, K., Zak, P., Viljanen, M., Lindström, M., Feldman, T. and Ostrovsky, M. (2016). Eye spectral sensitivity in fresh-and brackish-water populations of three glacial-relict *Mysis* species (Crustacea): physiology and genetics of differential tuning. *J. Comp. Physiol. A* **202**, 297–312.
- Dontsov, A. E., Fedorovich, I. B., Lindström, M. and Ostrovsky, M. A. (1999). Comparative study of spectral and antioxidant properties of pigments from the eyes of two *Mysis relicta* (Crustacea, Mysidacea) populations, with different light damage resistance. *J. Comp. Physiol. B* **169**, 157–164.
- Eronen, M., Glücker, G., Hatakka, L., van de Plassche, O., van der Plicht, J. and Rantala, P. (2001). Rates of Holocene isostatic uplift and relative sea-level lowering of the Baltic in SW Finland based on studies of isolation contacts. *Boreas* **30**, 17–30.
- Feldman, T. B., Dontsov, A. E., Yakovleva, M. A., Fedorovich, I. B., Lindström, M., Donner, K. and Ostrovsky, M. A. (2008). Comparison of antioxidant systems

- in the eyes of two *Mysis relicta* (Crustacea: Mysidacea) populations, with different light damage resistance. *Sens. Syst.* **22**, 1-8.
- Feldman, T., Yakovleva, M., Lindström, M., Donner, K. and Ostrovsky, M.** (2010). Eye adaptation to different light environments in two populations of *Mysis relicta*: a comparative study of carotenoids and retinoids. *J. Crustacean Biol.* **30**, 636-642.
- Glickman, R. D.** (2002). Phototoxicity to the retina: mechanisms of damage. *Int. J. Toxicol.* **21**, 473-490.
- Govardovskii, V. I., Fyhrquist, N., Reuter, T., Kuzmin, D. G. and Donner, K.** (2000). In search of the visual pigment template. *Vis. Neurosci.* **17**, 509-528.
- Hallberg, E.** (1977). The fine structure of the compound eyes of mysids (Crustacea: Mysidacea). *Cell Tissue Res.* **184**, 45-65.
- Insausti, T. C., Le Gall, M. and Lazzari, C. R.** (2013). Oxidative stress, photodamage and the role of screening pigments in insect eyes. *J. Exp. Biol.* **216**, 3200-3207.
- Johnston, I. A. and Dunn, J.** (1987). Temperature acclimation and metabolism in ectotherms with particular reference to teleost fish. *Symp. Soc. Exp. Biol.* **41**, 67-93.
- Jokela-Määttä, M., Pahlberg, J., Lindström, M., Zak, P. P., Porter, M., Ostrovsky, M. A., Cronin, T. W. and Donner, K.** (2005). Visual pigment absorbance and spectral sensitivity of the *Mysis relicta* species group (Crustacea, Mysida) in different light environments. *J. Comp. Physiol. A* **191**, 1087-1097.
- Kashiwagi, T., Meyer-Rochow, V. B., Nishimura, K. and Eguchi, E.** (1997). Fatty acid composition and ultrastructure of photoreceptive membranes in the crayfish *Procambarus clarkii* under conditions of thermal and photic stress. *J. Comp. Physiol. B* **167**, 1-8.
- Lindström, M. and Nilsson, H. L.** (1983). Spectral and visual sensitivities of *Cirolana borealis* Lilljeborg, a deep-water isopod (Crustacea: Flabellifera). *J. Exp. Mar. Biol. Ecol.* **69**, 243-256.
- Lindström, M. and Nilsson, H. L.** (1988). Eye function of *Mysis relicta* Lovén (Crustacea) from two photic environments. Spectral sensitivity and light tolerance. *J. Exp. Mar. Biol. Ecol.* **120**, 23-37.
- Loew, E. R.** (1976). Light, and photoreceptor degeneration in the Norway lobster, *Nephrops norvegicus* (L.). *Proc. R. Soc. Lond. Ser. B* **193**, 31-44.
- McNamara, J. C. and Torres, A. H.** (1999). Ultracytochemical location of Na<sup>+</sup>/K<sup>+</sup>-ATPase activity and effect of high salinity acclimation in gill and renal epithelia of the freshwater shrimp *Macrobrachium olfersii* (Crustacea, Decapoda). *J. Exp. Zool.* **284**, 617-628.
- Meyer-Rochow, V. B.** (2001). The crustacean eye: dark/light adaptation, polarization sensitivity, flicker fusion frequency, and photoreceptor damage. *Zool. Sci.* **18**, 1175-1197.
- Meyer-Rochow, V. B. and Lindström, M.** (1997). Light-induced photoreceptor sensitivity loss and recovery at 4°C and 14°C in *Mysis relicta* Lovén (Crustacea: Peracarida) from Pojoviken Bay (Finland). *Ann. Limnol.* **33**, 45-51. EDP Sciences.
- Nilsson, H. L.** (1982). Rhabdom breakdown in the eye of *Cirolana borealis* (Crustacea) caused by exposure to daylight. *Cell Tissue Res.* **227**, 633-639.
- Organisciak, D. T. and Vaughan, D. K.** (2010). Retinal light damage: mechanisms and protection. *Prog. Retinal Eye Res.* **29**, 113-134.
- Stavenga, D. G. and Hardie, R. C.** (2011). Metarhodopsin control by arrestin, light-filtering screening pigments, and visual pigment turnover in invertebrate microvillar photoreceptors. *J. Comp. Physiol. A* **197**, 227-241.
- Stephens, P. J.** (1985). The effects of temperature and acclimation on crustacean nerve-muscle physiology. *Biol. Bull.* **169**, 92-105.
- Wu, C.-S. and Kam, Y.-C.** (2009). Effects of salinity on the survival, growth, development, and metamorphosis of *Fejervarya limnocharis* tadpoles living in brackish water. *Zool. Sci.* **26**, 476-482.
- Wu, C.-S., Yang, W.-K., Lee, T.-H., Gomez-Mestre, I. and Kam, Y.-C.** (2014). Salinity acclimation enhances salinity tolerance in tadpoles living in brackish water through increased Na<sup>+</sup>, K<sup>+</sup>-ATPase expression. *J. Exp. Zool. A* **321**, 57-64.
- Zak, P. P., Lindström, M., Demchuk, J. V., Donner, K. and Ostrovsky, M. A.** (2013). The eye of the opossum shrimp *Mysis relicta* (Crustacea, Mysidae) contains two visual pigments located in different photoreceptor cells. *Dokl Biol. Sci.* **449**, 68-72.